

# Simple methods of voltage dip tracking – case study

Tomasz Tarasiuk

Gdynia Maritime University, Morska 81-87, 81-225 Gdynia, Poland

## ABSTRACT

The paper presents results of an experimental study of two methods of voltage dip tracking. The first is based on half cycle absolute peak value monitoring, whereas the second is based on low-pass filtration of squares of voltage samples. Both methods are devised for application in low-cost integrated circuits, dedicated to power quality monitoring. The two real voltage dips have been considered for the aim. The results are compared with the reference method recommended in IEC Std. 61000-4-30, based on calculation of the r.m.s. voltage refreshed each half cycle. Further, the application of the low-pass method for assessment small voltage variations is considered, both short term (r.m.s. voltage refreshed each half cycle) and long term (r.m.s. voltage calculated over 10 cycles of voltage fundamental component). The research confirmed sufficient accuracy of the method based on low-pass filtering for the class A of measurement.

**Section:** RESEARCH PAPER

**Keywords:** voltage short and long term variations, low-cost measurement, low-pass filtering

**Citation:** Tomasz Tarasiuk, Simple methods of voltage dip tracking–case study, Acta IMEKO, vol. 6, no. 4, article 13, December 2017, identifier: IMEKO-ACTA-06 (2017)-04-13

**Section Editor:** Konrad Jedrzejewski, Warsaw University of Technology, Poland

**Received** January 26, 2016; **In final form** November 15, 2017; **Published** December 2017

**Copyright:** © 2017 IMEKO. This is an open-access article distributed under the terms of the Creative Commons Attribution 3.0 License, which permits unrestricted use, distribution, and reproduction in any medium, provided the original author and source are credited

**Funding:** Ministry of Science and Higher Education under Grant DS/430/2017

**Corresponding author:** Tomasz Tarasiuk, e-mail: t.tarasiuk@we.am.gdynia.pl

## 1. INTRODUCTION

The problem of power quality in electric power networks is one of the hottest topics in electrical power engineering over recent years. Proliferation of non-linear loads and renewable energy resources have led to notorious voltage disturbances, like voltage and current waveform distortions, voltage dips etc. The intelligent metering and monitoring systems are necessary [1] to monitor power flow and various voltage and current parameters in numerous locations thorough the grid. However, the proper solutions have to be implemented, in order not to increase the cost of the whole infrastructure. In author's opinion, apart from high grade power quality analysers, a number of low-cost devices will be used, like instruments based on dedicated integrated circuits with fixed signal processing algorithms, Application Specific Integrated Circuits (ASICs). Fortunately, such low-cost ASICs are already available on "the shelf", e.g. Analog Devices *Single Phase, Multifunction Metering IC with Neutral Current Measurement ADE7953* [2] or Cirrus Logic *Single phase bi-directional Power/Energy IC CS5461A* [3]. They enable the measurement of voltage and current r.m.s. values, power and energy as well as dips or swells assessment. Although they are based on various processing principles, the

common feature of the devices is signal processing executed by fixed function digital signal processor (DSP) [2]. Among the applied algorithms, the input signal filtrations are used for different aims like: elimination of input channels offset, zero-crossing detection or r.m.s. values of the signals and active power measurements [2].

This paper is focused solely on the singular feature of these ICs, namely capacity of voltage dip or swell detection. There are several methods of dip detection and characterization, starting from simple solutions as: voltage peak value monitoring [4]-[8] or the traditional voltage r.m.s. value calculation [4]-[8], up to more complex solutions based on d-q transformation [4], [9], short time Fourier transform [5], wavelet transform [4], [5], [8], [10], [11], Kalman filtering [4], [5], [12] or a combination of both wavelet and Kalman filtering [5], to name the most popular. The comparative study on chosen methods performance can be found e.g. in [6] and [8]. Unfortunately, the last group of methods lacks simplicity required for implementation in simple, low cost and low energy consuming ASICs due to complex models and/or the necessity of implementation of a number of conditional and branching operations. Therefore, the simpler solutions are used in ASICs.

For instance, the manufactures of above mentioned ASICs [2], [3] use the method based on peak value monitoring. Simply put, if the magnitude of the instantaneous voltage (its absolute value) is below the pre-defined threshold value, a dip is detected. Similarly, the swell is to be identified if the absolute value of the magnitude of the instantaneous voltage is above the pre-defined threshold. The method is simple and easy to implement in ASICs. But the downside of the solution is a notorious impact of noise and distortions of the voltage on the outcome of the dip or swell identification [4], [8]. This can be avoided by superseding this method by an equally simple one based on low-pass filtering of the squares of the input voltage samples, like the method already used by some manufacturers for the r.m.s. value of voltage and current measurements [2], although not used for dip and swell identification. Therefore, the paper aim is to explore the possibility of using this solution in its simplest form, which can be easily applied in ASICs, for dip and swell identification. It is compared with the above mentioned method based on the absolute value of instantaneous voltage monitoring. Both solutions are evaluated against the reference measurement procedure laid in IEC Standard 61000-4-30 for Class A measurements, based on the measurement of the r.m.s. voltage over 1 cycle, commencing at a fundamental zero crossing, and refreshed each half-cycle  $U_{rms(1/2)}$  [13]. This is recommended for voltage dips, swell and interruption detection and evaluation [14]. It has to be added that some documents use the term sag as synonym to the term dip [2], [3], [14]. But since the term dip is used by IEC, it will be used consequently thorough this paper.

Finally, the paper presents a comparative study of the performance of these two methods. The first method is based on monitoring the voltage peak value. The second method is based on the r.m.s. voltage value determined by low pass filtering. Because the idea behind the paper is to use real cases for the method's performance assessment, results obtained by both solutions are compared against quantity values provided by the reference measurement procedure to assess the measurement trueness of the measured quantity values obtained from analysed procedures [15]. The reference procedure is described in detail in Section 2. This section includes also basic information about limitations of the standard procedure. All subsequent analyses of experimental data are based on two voltage dips registered in real microgrids, namely the network of a sensitive data centre during its island operation mode as well as a marine microgrid, a network of a ferry, during switch-on of the high power electric motor (for driving the bow thruster). Further, another marine network with high distortion (voltage THD=11.8 %) and voltage and frequency modulation was considered for determining the method's performance for tracking short-term voltage variations. The paper is the extended and updated version of the work presented during the XXI IMEKO World Congress, 2015, Prague, Czech Republic [16].

## 2. STANDARD FRAMEWORK – REFERENCE MEASUREMENT PROCEDURE

The voltage dip is defined as the sudden decrease in r.m.s. value of the supply voltage to a value between 10 % and 90 % of the declared voltage (in another standard it is 1 % to 90 % [17]) for durations from 0.5 cycles to 1 min [14]. A voltage dip is to be described by a pair of data: residual voltage (sometimes dip's depth) and its duration [13]. The residual voltage is the

lowest r.m.s. value of the voltage during the considered event, whereas duration is the time difference between the start time (falling of r.m.s. voltage below the dip threshold) and end the time (increase of r.m.s. voltage above the dip threshold plus hysteresis typically equal to 2 % of declared voltage) [13]. In some cases, the voltage dip is followed by a voltage peak (small swell), e.g. during a asynchronous motor start up in the microgrid [18]. Typically, a voltage swell is monitored by the same methods like a voltage dip, e.g. voltage instantaneous values [2] or r.m.s. values [13].

It was mentioned above that for Class A measurements the considered r.m.s. voltage should be calculated over 1 cycle, commencing at a fundamental zero crossing, and refreshed each half-cycle. It is designated as  $U_{rms(1/2)}$  [13] and it includes all components like: harmonics, interharmonics, etc. [13]. It has to be added that Class S has been defined at the IEC Standard 61000-4-30 as well. For this class the dip assessment is to be carried out in a similar way like the above described but the voltage r.m.s. value can be refreshed each cycle. Manufacturers of measuring instrument should specify which method is used [13].

Finally, the r.m.s. value is to be calculated as square root of the mean value of squares of the voltage samples registered over the considered time interval, like required in IEC Standard 61557-12 [19]. The evaluation of a real dip carried out by the method devised for Class A is used in this paper as a reference measurement procedure for evaluations of the other methods, including whole voltage shape assessment during the considered processes, namely bulk load startup in two investigated microgrids and resulted dips. Next, it is compared with the same shape determined by the other simple method under investigation based on monitoring the voltage peak value.

It must be firmly stressed that the standard approach is contested by some authors. For instance, in [6], the detailed analysis of the standard method's performance for short dips (duration below two cycles) was presented. Authors of [6] pointed out the ambiguity in determining the dip parameters, both duration and residual voltage, by the standard solution for such a short duration phenomenon. This is chiefly related to synchronization based on fundamental zero crossing [6], [8]. The proposed solution can be based on determining the rms value of the voltage over a one-cycle sliding window and computing the rms value at every sampling point [6], [7]. However, the solution entails higher computational burden for ensuring that the window length fits the actual fundamental period [6]. Another frequently investigated solution is tracking the energy of the band 0-100 Hz after wavelet transformation for detection of short duration dips [10] but this also entails an increase in computational complexity.

Next, the standard method has another limitation, namely it "does not provide information about the phase angle of voltage supply during the event, which could be of interest for some applications" [8]. Reference [20] lists seven dip characterization methods, including four which require phase angle information.

Despite the above mentioned drawbacks of the standard method, it arguably remains one of the most popular due to its simplicity and sufficient performance for a number of most common applications.

## 3. THE METHODS UNDER INVESTIGATION

Notwithstanding its simplicity, the application of the above described standard procedure for dip detection and evaluation

can be inconvenient in simple low-cost devices, due to some requirements for hardware resources of the measuring instrument. In shorthand, it requires storing of voltage samples for at least one cycle, conditional operation, some data address generating, etc. Obviously, it can be easily implemented in digital signal processors (DSPs) but not necessary in low-cost dedicated ASICs. Therefore, manufacturers of low-cost measuring devices implement other principles of dip detection and evaluation [2], [3]. It is permissible for Class B measurements if the manufacturer specifies the method used for the aim [13]. So, the paper explores the performance of two arguably simplest methods of voltage dip detection and characterization, which can be used for less demanding applications and both easy to apply in ASICs.

### 3.1. Dip measurement based on voltage peak value tracking

Arguably, the simplest solution of the considered problem is detection of time instants when the absolute value of the voltage falls below the programmable threshold [2], [3]. This feature is easy to implement in ASICs. Simply, the dedicated peak register is updated with a new instantaneous voltage value every time that the absolute value of the voltage sample exceeds the sample value already stored in the register. The register can be cleared after reading [2], which can be synchronized with the voltage fundamental component zero-crossing in order to determine the end of each half-cycle. This feature enables continuous recording the maximum value of the voltage waveforms for each half cycle. Apart of its simplicity, the obvious disadvantage of the solution is the above mentioned possible impact of voltage distortions or noise [4], [8], since for distorted signals one cannot conclude on its r.m.s. value basing only on the maximum value of the voltage waveforms. It will be proved below that even in the case of low distortion, the results of dip analysis by the method can differ noticeably from the reference method.

### 3.2. Dip measurement based on low-pass filtering of squares of voltage samples

The standard dip assessment method is based on the determination of the voltage r.m.s. value over one cycle. It can be easily noted that

$$U_{rms} = \sqrt{\frac{1}{N} \cdot \sum_{k=0}^{N-1} u_k^2} \approx \sqrt{LPF(u_k^2)} \quad (1)$$

where  $N$  is the number of voltage samples recorded over an integer number of cycles (in fact one cycle for dip assessment),  $u_k$  is the voltage sample, LPF is a low-pass filter

The solution consists in superseding the mean filter with  $N$  coefficients (each with value of  $1/N$ ) by another LPF filter. Since  $N$  varies depending on the instantaneous frequency it seems much easier to implement in ASICs a low-pass filter with a constant number of coefficients. Because of the ripples of the LPF output, the reading should be synchronised with the voltage fundamental component zero-crossing. It is determined after low-pass filtering of the voltage samples by another LPF. The algorithm [2] after some modifications is shown in Figure 1. It should be added that the solution is applied using an *ADE7953* [2] for the r.m.s. measurement but not for dip detection and evaluation.

The signal processing path shown in Figure 1 can be used for both: measuring the r.m.s. value of the voltage during steady-state as well as dip monitoring. The reading is to be carried out after each zero-crossing of the voltage fundamental

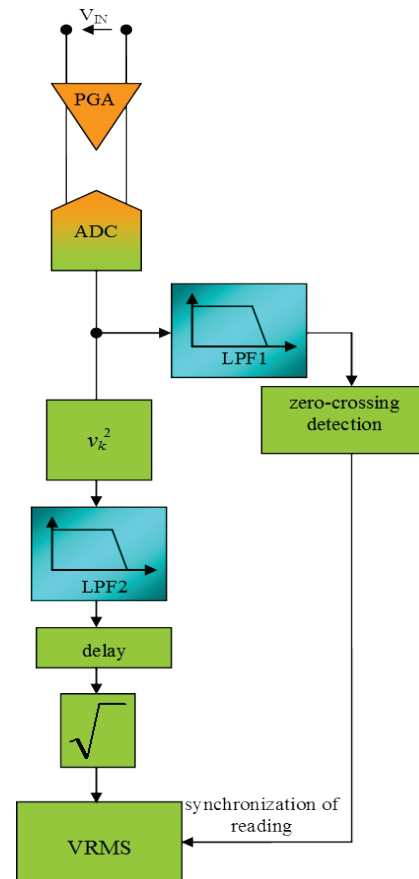


Figure 1. Block diagram of the signal processing path for the measurement of r.m.s. voltage, including dip detection and evaluation.

component, similar as in the case of the  $U_{rms(1/2)}$  measurement. This value is used directly to the dip or swell detection and evaluation. Namely, it is to be compared with the assumed threshold level, once again similar as in the case of the standard method. In order to obtain a 10-cycles rms voltage, accumulation of  $U_{rms(1/2)}$  and averaging is necessary. The block “delay” shown in Figure 1 is to account for the LPF1 and LPF2 characteristics (group delays of both filters). It means shifting of the samples of the LPF2 output. It depends on the actual power frequency. So, adaptation of the shift is to be performed. A simpler solution is to use constant sample shifts related to the rated power frequency but it can impact the accuracy of the proposed solution if used in islanded microgrids due to possible power frequency changes.

## 4. RESULTS OF EXPERIMENTAL RESEARCH

The real examples are used for this paper’s purpose. So, the research consisted in voltage samples registration in real networks and subsequent processing by various signal processing methods. A National Instruments controller PXIe-8106 equipped with two data acquisition boards PXIe-6124 was used for voltage samples recording in an office building. The analog input channel consisted of CV3-1500 LEM voltage transducers and LTC 1564 anti-aliasing filters. The cut-off frequency of the anti-aliasing filters was equal to 10 kHz. In the case of marine systems, data acquisition board PCI703-16/A Eagle Technology, a resistive voltage divider and isolation amplifiers ISO 124 of Burr Brown were used. The cut-off frequency of the anti-aliasing filter was equal to 3.5 kHz.

Finally, the momentary voltages for dip detection are calculated by both investigated methods. The results obtained by analysis of the voltage local peak values (like used in [2] and [3]) are designated as  $U_{ABS}$ . The recorded absolute values of the voltage waveform are divided by  $\sqrt{2}$  in order to obtain the voltage r.m.s. value and subsequently to compare with the reference method. The results calculated by voltage samples squaring and low-pass filtering of the result are designated as  $U_{L_{PF}}$ . It represents the r.m.s. voltage momentary values. For the paper purpose, a third order Butterworth filter is used with various cut-off frequencies. It has been mentioned (see Figure 1) that, in order to diminish the effect of ripples of the filter output, its reading is to be synchronised with the fundamental component zero-crossing. Zero-crossing of the fundamental component of the voltage is determined after low-pass filtering by another third order Butterworth filter, but with higher cut-off frequency equal to 80 Hz. Such a solution is recommended in the IEC 61000-4-30 standard for diminishing the impact of higher frequency components. The cut-off frequency is chosen after [2]. To compare the differences between the considered methods and the reference method, the square root of the mean value of squares of the differences is calculated by:

$$SQR(diff) = \sqrt{\frac{1}{N} \sum_{k=0}^{N-1} (U_{meth_k} - U_{rms(1/2)_k})^2} \quad (2)$$

where  $U_{meth}$  is the method under investigation ( $U_{ABS}$  or  $U_{L_{PF}}$ ),  $N$  is the number of considered half cycles for the dip assessment. It is assumed that  $N=146$  starting at the dip beginning.

#### 4.1. Dip in emergency power system of office building

The voltage recording took place in the network of an office building that contained a very important data centre and sensitive for power quality disturbances. Particularly, interruptions can lead to severe consequences. Therefore, it was equipped with two UPSs and two generators driven by diesel engines for power backup. The network rated voltage was equal to 230 V and the rated frequency 50 Hz. The whole research was carried out during the object island operation mode, due to suspicion of power quality problems during the mode. Various parameters of voltage and currents were analysed in various points of the system. During the investigation the process of switching-on the bulk load was recorded. The waveform of the recorded voltage is presented in Figure 2.

It is easily discernible that the process of switching bulk load on in the power network of the data centre causes a voltage dip up to 85 % of the rated voltage followed by a small voltage swell. It is only 101.6 % of the rated voltage but approximately above 5 % of the registered mean steady-state voltage, which was approximately equal to 96.8 % of the rated voltage (230 V). Nevertheless, this phenomenon is considered as well, in order to properly assess the methods under investigation. The details of  $U_{rms(1/2)}$  calculated according to the IEC 61000-4-30 standard and the resulting voltage shape are shown in Figure 3.

Obviously, the processes of switching bulk load on in microgrids cause voltage changes and concurrent momentary frequency changes. For the considered example, the lowest momentary frequency understood as reciprocal of fundamental cycle is equal to 48.61 Hz followed by a frequency increase up to 51.51 Hz. Typically, standards related to marine microgrids, e.g. [21], [22] deal with the phenomenon, but it has not been analysed for the paper's aim. However, both investigated

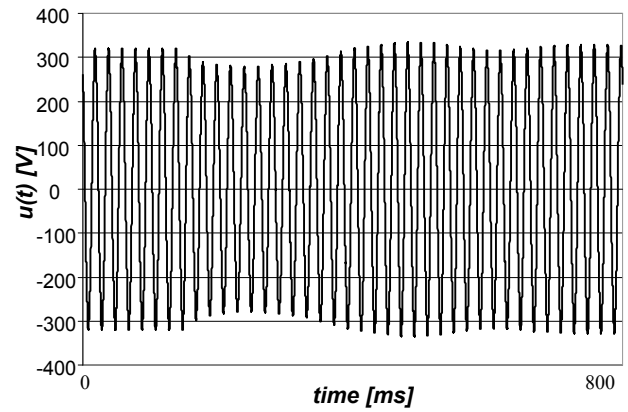


Figure 2. Voltage waveform during switching bulk load on in a power network of data centre during island operation.

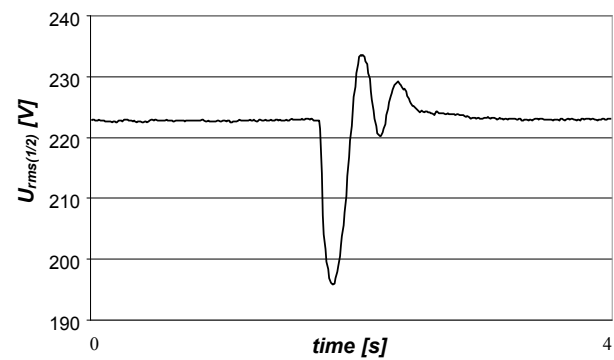


Figure 3. Variations of  $U_{rms(1/2)}$  value (reference method) during switching bulk load on in a power network of a data centre during island operation; residue voltage equals 195.86 V (85.16 % of  $U_{rated}$ ), dip duration 18 half cycles, swell equals 233.58 V.

methods, which depend to some respect on the fundamental component zero-crossing, enable concurrent assessment of momentary frequency changes, including their value and duration. In fact, assessment of rapid power frequency changes in marine systems is similar as in the case of voltage dip assessment [21], [22].

Finally, the results of the calculation of parameter pairs for the dip assessment (residue voltage  $U_{min}$  and duration), completed by the r.m.s. value of the mini-swell  $U_{max}$  voltage that followed the considered dip are shown in Table 1. Moreover, results of determining  $SQR(diff)$  for each of the methods are presented in the table as well.

Analysis of results in Table 1 leads to the conclusion that results of dip shape assessment for filters with cut-off frequencies from 15 Hz up to 19 Hz lead to comparable results. Observed minor differences can be neglected. The lowest  $SQR(diff)$  value is obtained for a filter with cut-off frequency 17 Hz. The analysis confirms that the  $U_{ABS}$  method leads to worse results than the method based on low-pass filtering of the squares of voltage samples for most of the used filters.

Next, the capability of tracking the voltage shape for each of the methods is assessed. It is carried out by determining the differences between  $U_{L_{PF}}$  and  $U_{rms(1/2)}$  (they are graphically presented in Figure 4 for L<sub>PF</sub>2 with cut-off frequency equal to 17 Hz) and the differences between  $U_{ABS}$  and  $U_{rms(1/2)}$ . The results of comparison are shown in Figure 5.  $SQR(diff)$  values for these examples are given in Table 1 as well.

Table 1. Calculation results of dip (duration and  $U_{min}$ ) and swell ( $U_{max}$ ) parameters completed by  $SQR(diff)$ .

	$f_{cutoff}$	half cycl.	$U_{min}$		$U_{max}$	$SQR(diff)$
			[V]	[%]	[V]	[V]
$U_{rms(1/2)}$		18	195.86	85.16	233.58	---
$U_{ABS}$		17	197.6	85.91	236.47	3.26
$U_{LPF}$	1 Hz	---	212.87	92.55	226.99	6.23
	2 Hz	15	203.64	88.52	228.20	3.51
	3 Hz	17	198.28	86.20	232.53	1.72
	4 Hz	17	196.26	85.33	233.46	1.13
	5 Hz	17	195.20	84.87	233.68	0.88
	6 Hz	17	194.99	84.77	233.69	0.85
	7 Hz	18	194.96	84.76	233.72	0.68
	8 Hz	17	195.16	84.85	233.71	0.55
	9 Hz	18	195.43	84.97	233.66	0.61
	10 Hz	17	195.69	85.08	233.69	0.53
	11 Hz	18	195.87	85.16	233.67	0.36
	12 Hz	18	195.98	85.20	233.66	0.45
	13 Hz	18	196.00	85.20	233.67	0.64
	14 Hz	18	195.93	85.17	233.67	0.51
	15 Hz	18	195.87	85.16	233.65	0.35
	16 Hz	18	195.83	85.14	233.62	0.23
	17 Hz	18	195.82	85.14	233.59	0.20
	18 Hz	18	195.83	85.14	233.58	0.25
	19 Hz	18	195.87	85.16	233.59	0.34
	20 Hz	18	195.87	85.16	233.59	0.88

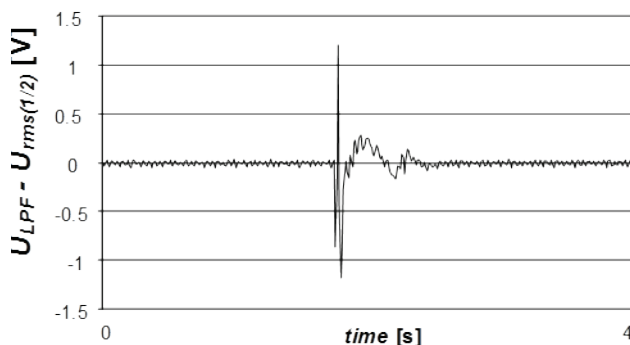


Figure 4. The differences between r.m.s. value of voltage calculated by filtering of square samples  $U_{LPF}$  (LPF2 cur-off frequency=17 HZ) and reference method  $U_{rms(1/2)}$ .

Comparison of Figures 4 and 5 once again reveals clear superiority of the first solution, i.e.  $U_{LPF}$ . The difference between the considered method and the reference method does not exceed 1.2 V. Maximal values are observed for the dip beginning. Similar differences for the  $U_{ABS}$  method reach values above 4 V. The reason is distortion of the investigated voltage, although with a relatively low level. The value of the voltage THD was equal to 3.13 % prior to the considered dip and 3.26 % after the dip. It can be noted that even this small increase leads to a significant increase in differences between  $U_{ABS}$  and  $U_{rms(1/2)}$  (see Figure 5). The differences increase nearly two times

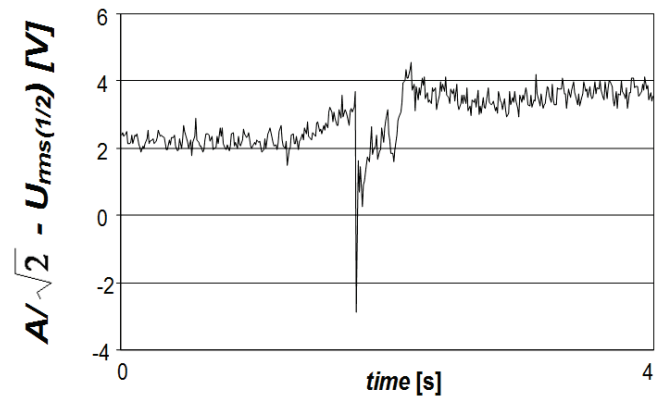


Figure 5. The differences between rms value of the voltage calculated on the basis of the absolute peak value of voltage  $U_{ABS}$  and reference  $U_{rms(1/2)}$ .

under steady-state conditions: before and after dip. The main reason is the increase of the 5<sup>th</sup> harmonic content by 0.19 % of the fundamental component, completed by a phase shift of some harmonics in relation to the fundamental component after the dip and a resulting increase in the voltage maximal instantaneous value.

#### 4.2. Dip in power system of a ferry

The second example concerns the dip caused by switching on the high power electric motor with rated power 1.72 MW on board a ferry with a 6.6 kV - 60 Hz system. The motor start prior to the ship manoeuvring has led to a severe voltage dip, namely the voltage dropped below the permissible limit -20 % of the rated voltage [21], [22].

Similar as in the previous example, the dip parameters are determined by the two investigated methods. The waveform of the recorded voltage is presented in Figure 6 and the details of  $U_{rms(1/2)}$  calculated according to the IEC 61000-4-30 standard and the resulting voltage shapes are shown in Figure 7. The calculation results of the parameter pairs for the dip assessment (residue voltage  $U_{min}$  and duration), completed by the r.m.s. voltage of the mini-swell  $U_{max}$  that followed the considered dip are shown in Table 2 and the differences between  $U_{LPF}$  and  $U_{rms(1/2)}$  and the differences between  $U_{ABS}$  and  $U_{rms(1/2)}$  are given in Figures 8 and 9, respectively

Once again, analysis of the above results leads to the conclusion that application of LPF filters with cut-off frequencies 12-20 Hz gives satisfactory results. The solution superiority over  $U_{ABS}$  method is clearly visible, despite the fact that for the ferry voltage THD hardly exceeded 1.2 %.

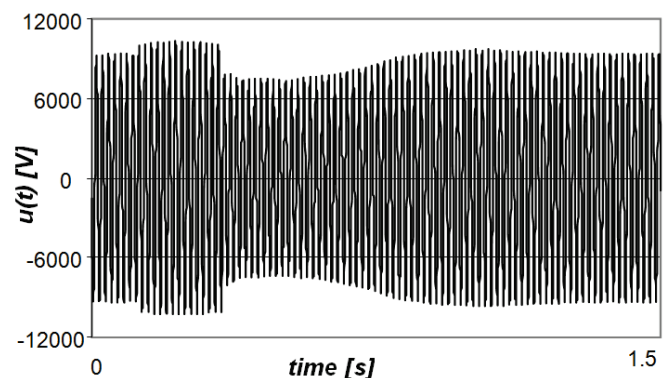


Figure 6. Voltage waveform during switch-on of the thruster in power network of ferry.

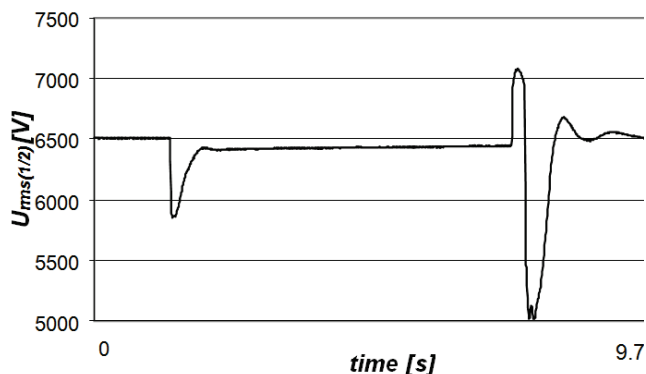


Figure 7. Variations of  $U_{rms(1/2)}$  (reference method) during switching of the thruster onboard a ferry; residue voltage equals 5015 V (75.98 % of  $U_{rated}$ ), dip duration equals to 51 half cycles, swell equals to 7083.1 V.

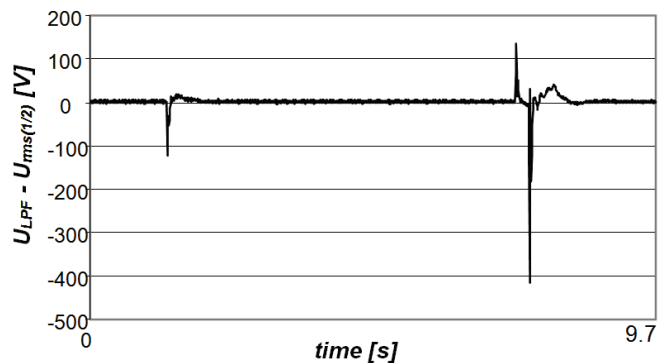


Figure 8. The differences between the r.m.s. value of voltage calculated by filtering of square samples  $U_{LPF}$  (LPF2 cut-off frequency=17 Hz) and reference method  $U_{rms(1/2)}$ .

Table 2. Results of calculation of dip (duration and  $U_{min}$ ) and swell ( $U_{max}$ ) parameters completed by  $SQR(diff)$ .

	$f_{cutoff}$	half cycl.	$U_{min}$		$U_{max}$	$SQR(diff)$
			[V]	[%]		
$U_{rms(1/2)}$		51	5015.0	75.98	7083.1	---
$U_{ABS}$		49	5211.6	78.96	7299.6	170.03
$U_{LPF}$	1 Hz	52	5554.2	84.15	6671.4	326.89
	2 Hz	48	4990.2	75.61	6958.7	146.99
	3 Hz	49	4884.4	74.01	7083	108.95
	4 Hz	49	4891.1	74.11	7105.6	87.96
	5 Hz	50	4918.0	74.52	7111.5	76.13
	6 Hz	50	4926.7	74.65	7109.9	64.24
	7 Hz	50	4929.8	74.69	7105.7	55.97
	8 Hz	50	4938.7	74.83	7100.5	51.63
	9 Hz	51	4953.1	75.05	7093.8	46.56
	10 Hz	52	4974.3	75.38	7086.9	42.23
	11 Hz	51	4993.7	75.66	7080.4	38.26
	12 Hz	51	5016.9	76.01	7074.7	42.65
	13 Hz	51	5015.5	75.99	7083.1	33.88
	14 Hz	51	5014.9	75.98	7083.1	28.86
	15 Hz	51	5013	75.95	7079.6	28.70
	16 Hz	52	5012.8	75.95	7080.8	32.15
	17 Hz	51	5014.3	75.97	7082.0	38.19
18 Hz	51	5013.6	75.96	7083.3	28.18	
19 Hz	51	5013.6	75.96	7084.2	22.58	
20 Hz	51	5014.8	75.98	7085.9	18.43	

### 4.3. Voltage variations tracking in the system with high level of voltage distortion

The voltage registered on board of a chemical tanker was chosen for the assessment of the performance under significantly distorted conditions. The vessel is equipped with a shaft generator working on main bus bars via a power converter to obtain a constant frequency. The system rated voltage was 440 V and rated frequency 60 Hz. The voltage waveform registered in the system of the chemical tanker is shown in Figure 10. For the assessment, the measurement results of the

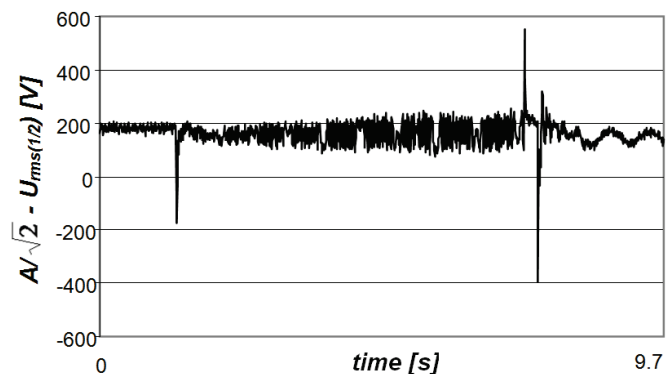


Figure 9. The differences between the rms value of the voltage calculated on the basis of the absolute peak value of voltage  $U_{ABS}$  and reference  $U_{rms(1/2)}$ .

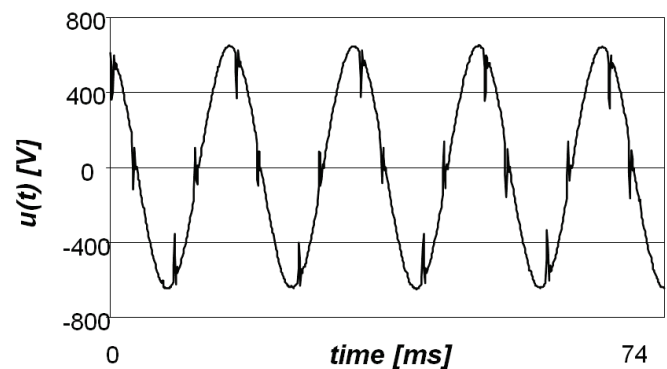


Figure 10. Voltage waveform in a marine system with a shaft generator working via a power converter, THD=11.8 %.

voltage modulation by low-pass filtering  $U_{LPF}$  and by the  $U_{rms(1/2)}$  method were compared. It is to exemplify the capability of tracking of the voltage variations by the  $U_{LPF}$  method. It must be stressed that the considered case is very hard to analyze because of concurrent presence of significant waveform distortions as well as fundamental voltage and frequency modulations shown in Figure 11. The instantaneous frequency and voltage for Figure 11 are calculated by a zoom-DFT with Kaiser window, refreshed every 0.5 ms and with a frequency resolution 0.001 Hz. For this case, a similar modulation was observed for harmonics, e.g. the r.m.s. of the 5<sup>th</sup> harmonic varied between 15 and 25 V.

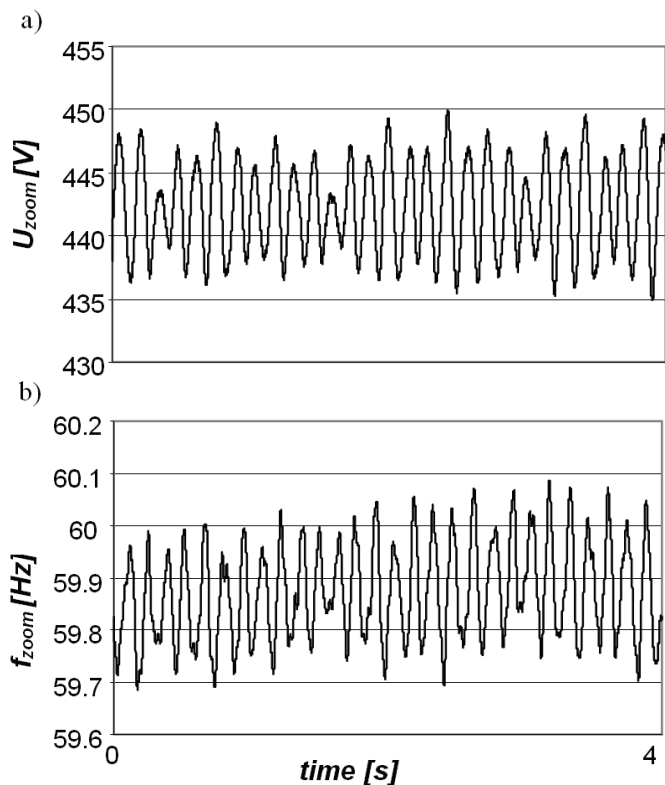


Figure 11. Fluctuations of voltage (a) and its frequency (b) on board of chemical tanker determined by zoom-DFT.

The two voltage tracking methods are graphically compared in Figure 12, for a steady-state condition. Assumed cut-off frequency of LPF2 filter is equal to 17 Hz.

Analysis of Figure 12 once again indirectly proves that the  $U_{LPF}$  method would be appropriate for the considered aim, namely tracking of voltage short-term variations, including voltage dip or swell detection and evaluation, even in the case of heavily distorted signals.

Finally, it has to be added that the r.m.s. value of voltage over 10 or 12 cycles time interval (depending on the power system's rated frequency) should be calculated for the assessment of magnitude of the supply voltage (apart from dips and swells detection) [13]. Because it would be unwise to design a separate signal processing path for the 10 or 12 cycles r.m.s. value determination, it seems that the simplest solution would

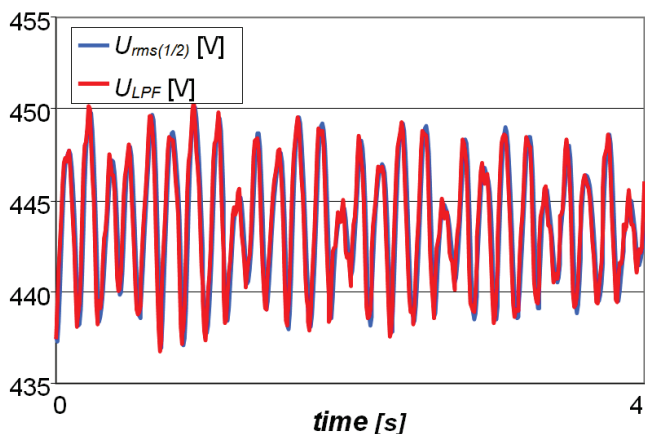


Figure 12. Comparison of tracking capabilities of short-term small voltage variations by  $U_{LPF}$  method with  $U_{rms(1/2)}$  method.

be determining the average value of readings of the LPF2 filter over a specified number of cycles. It can easily be implemented in ICs. To assess the accuracy of the solution, the average values of twenty or twenty four consecutive readings of the LPF2 filter with cut-off frequency equal to 17 Hz is determined for the office building (50 Hz system) and the chemical tanker (60 Hz system), respectively. They are graphically (Figure 13) compared with respective r.m.s. values determined for the very same time interval (exactly 10 cycles) by the reference method.

The analysis of the results presented in Figures 4, 8, 12 and 13 clearly indicates that the same signal processing path can be easily used for assessing voltage dips and swells as well as determining 10/12 cycles voltage magnitude after simple averaging. For example, the maximum difference between reference 10/12 cycle r.m.s. value and the respective value determined by averaging the LPF2 readings (cut-off frequency 17 Hz) is below 0.02 V for the case presented in Figure 13(a) and it is below 0.5 V for the case presented in Figure 13(b). The value of  $SQR(diff)$  is below 0.01 V for the former case and 0.3 V for the latter case.

## 5. CONCLUSIONS

The paper aim was the investigation of some simple algorithms for dip or swell detection and evaluation, easily applicable in low-cost ICs dedicated to multifunction electricity

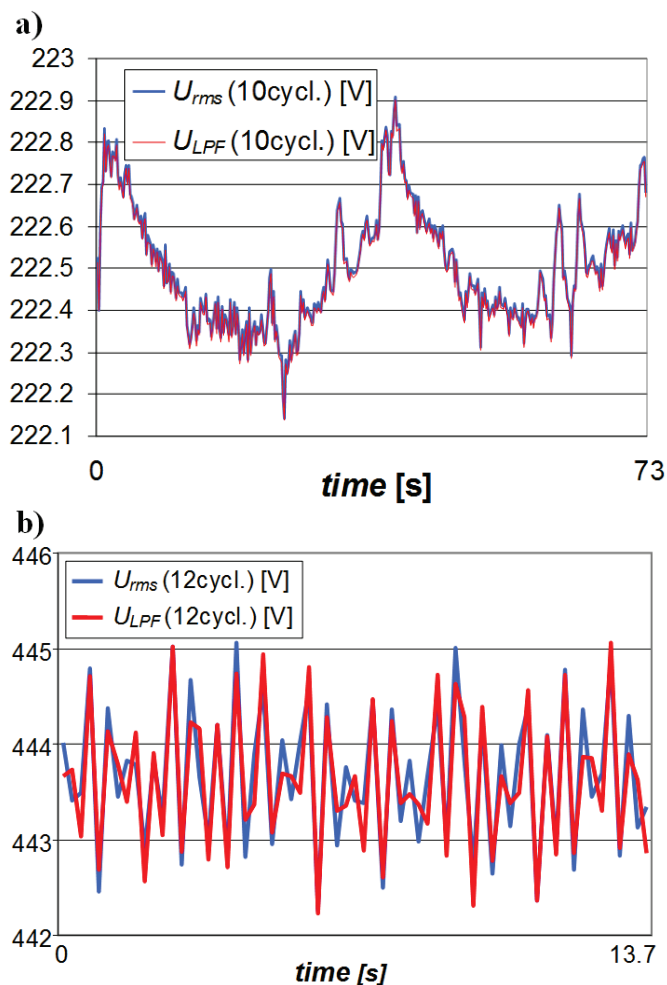


Figure 13. Comparison of reference r.m.s. value calculated over 10 or 12 cycles of input voltage and respective value of averaged LPF2 readings over the same time interval, (a) emergency supply of the office building, (b) bow thruster subsystem with non-linear load.

parameters measurements. It was proved that the method of signal processing based on low-pass filtering of the input voltage samples is more suitable for the aim than the commonly used method based on absolute values of the momentary voltage peak. In the latter case ( $U_{ABS}$  method) the significant impact of voltage distortions on the measurement accuracy can be observed. It is true even for slightly distorted signals, which are rather norm than exception in nowadays power systems.

Therefore, using the method based on low-pass filtering is arguably a better solution. Since it is already used for r.m.s. value estimation by the same ICs, it requires only some design modification, but special attention has to be paid to the cut-off frequency and group delay of implemented LPFs. The used cut-off frequency has to be increased in comparison with that currently used in ICs [2] but it inevitably leads to an increase in ripples of the filter output. Fortunately, the ripples impact is limited, if synchronisation of reading with voltage zero crossings is implemented. The resulting overall accuracy is better than in the case of the hitherto used solution, based on tracking of the absolute instantaneous value of the input voltage. Moreover, the reading of the used LPF2 filters can be used for determining the 10-cycles voltage magnitude with good accuracy after simple averaging. It simplifies the IC design, since the same signal processing path can be used for both aims, dip detection and the 10-cycles voltage magnitude measurement. Currently it is determined by two separate signal processing paths, in dedicated ICs with fixed DSP.

It has to be added that the solution based on low-pass filtering was devised for low-cost and low power consumption applications, with sufficient accuracy for trouble-shooting applications, like defined in the IEC Standard 61000-4-30 [13]. Its application for contractual purposes will require additional research, particularly for other voltage shapes during dips.

Next, the cut-off frequency of the applied LPF2 filter has to be carefully chosen, since it can affect the uncertainty of the method. If it is too low, it results in an increase in response time and the assessed residue voltage would be higher than the real one. This can affect the accuracy of determining the residue voltage during very short dips. However, a too high cut-off frequency would lead to an increase of ripples of the filter output and increase in the measurement uncertainty since reading exactly at the moments of zero-crossing is hardly possible. In fact, the results are affected by both LPF1 and LPF2 characteristics. Their correction can assume discrete values with a resolution equal to the sampling period, since delay means shifting samples of the LPF2 output. So, the accuracy of correction of the group delay for the respective filters is in the range of  $\pm 0.5 T_s$  ( $T_s$  – sampling period, which for the considered research equals 40  $\mu$ s for the office building and 95  $\mu$ s for the two later cases, namely the marine microgrids). The remaining factors influencing measurement uncertainty are the same as considered for typical performance monitoring and measuring devices and discussed in standard [19]. Particularly, the limitation of the method based on low-pass filtering is the necessity of synchronisation of the reading with the fundamental zero crossing. However, this is also a limitation of the solution based on the peak value, which can be determined once every half cycle.

Nevertheless, the research carried out for two various dip cases and completed by research of modulated, significantly distorted voltages (network of chemical tanker) proved to have good accuracy of the proposed solution, even under such unfortunate circumstances. The maximum difference between

the reference method (for 12 cycles time interval) and the described proposal hardly exceeded 0.11 % of the voltage rated value.

Summing up, in author's opinion, the proposed solution based on a simple low-pass filtering gives acceptable accuracy for less demanding applications and can be used for everyday monitoring of power systems performance. However, for more demanding or legal purposes other, more complex solutions, for instance mentioned in the introduction, should be considered.

## REFERENCES

- [1] EUROPEAN COMMISSION, "Communication From the Commission to the European Parliament, the Council, the European Economic and Social Committee and the Committee of the Regions, Smart Grids: from innovation to deployment." COM(2011) 202 final, Brussels, 12.4.2011.
- [2] Analog Devices, "Single Phase, Multifunction Metering IC with Neutral Current Measurement ADE7953", Data Sheet, 2011-2013.
- [3] Cirrus Logic, "Single phase bi-directional Power/Energy IC CS5461A", Data Sheet, 2011.
- [4] A. Khoshkbar Sadigh, K.M. Smedley, "Fast and precise voltage sag detection method for dynamic voltage restorer (DVR) application", *Electric Power Systems Research*, vol. 130, 2016, pp. 192–207.
- [5] E. Perez, J. Barros, "A Proposal for On-Line Detection and Classification of Voltage Events in Power Systems", *IEEE Trans. on Power Delivery* vol. 23, no. 4, 2008, pp. 2132-2138.
- [6] D. Gallo, C. Landi, M. Luiso, E. Fiorucci, "Survey on voltage dip measurements in standard framework", *IEEE Trans. on Instrumentation and Measurement*, vol. 63, no. 2, 2014, pp. 374-387.
- [7] M. Bollen, I. Gu, "Signal processing of power quality disturbances", New York, USA, Wiley, 2006.
- [8] A. Moschitta, P. Carbone, C. Muscas, "Performance Comparison of Advanced Techniques for Voltage Dip Detection", *IEEE Trans. on Instrumentation and Measurement*, vol. 61, no. 5, 2012, pp. 1494-1502.
- [9] O. Hua, B. Le-ping, Y. Zhong-lin, "Voltage Sag Detection Based on dq Transform and Mathematical Morphology Filter", *Procedia Engineering*, vol. 23, 2011, pp. 775 – 779.
- [10] M. Apraiz, J. Barros, R. Diego, "A real-time method for time-frequency detection of transient disturbances in voltage supply systems", *Electric Power Systems Research*, vol. 108, 2014, pp. 103– 112.
- [11] J. Decanini, M. Tonelli-Neto, F. Malange, C. Minussi, "Detection and classification of voltage disturbances using a Fuzzy-ARTMAP-wavelet network", *Electric Power Systems Research*, vol. 81, 2011, pp. 2057– 2065.
- [12] E. Pérez, J. Barros, "An extended Kalman filtering approach for detection and analysis of voltage dips in power systems", *Electric Power Systems Research*, vol. 78, 2008, pp. 618–625.
- [13] IEC Standard 61000-4-30, "Testing and Measurement Techniques – Power Quality Measurement Methods", 2015.
- [14] IEEE Standard 1159-2009, "IEEE Recommended Practice for Monitoring Electric Power Quality", 2009.
- [15] Joint Committee for Guides in Metrology "International vocabulary of metrology – Basic and general concepts and associated terms," 3rd edition, JCGM 200:2012.
- [16] T. Tarasiuk, "Comparative study on chosen methods of voltage dip tracking based on real example", XXI IMEKO World Congress "Measurement in Research and Industry" August 30 – September 4, 2015, Prague, Czech Republic.
- [17] EN Standard 50160, "Voltage characteristics of electricity supplied by public distribution networks", 2007.
- [18] A. Vicenzutti, D. Bosich, G. Giadrossii, G. Sulligoi, "The role of voltage controls in modern all-electric ships", *IEEE*

- Electrification Magazine, vol. 3, no. 2, 2015, pp. 49-65.
- [19] IEC Standard 61557-12, “Electrical safety in low voltage distribution systems up to 1000 V a.c. and 1500 V d.c. – Equipment for testing, measuring or monitoring of protective measures – Part 12: Performance measuring and monitoring devices (PMD)”, 2007.
- [20] Y. Wang, M. Bollen, A. Bagheri, X. Xiao, M. Olofsson, “A quantitative comparison approach for different voltage dip characterization methods”, *Electric Power Systems Research*, vol. 133, 2016, pp. 182–190.
- [21] DET NORSKE VERITAS, “Rules for classification of ships / high speed, light craft and naval surface craft. Electrical installations”, Part 4, Chapter 8, 2011.
- [22] IEEE Std. 45-2002, “IEEE Recommended Practice for Electrical Installations on Shipboard”, 2002.